Contactless Power Transfer System combined with Linear Electric Machine

Ji-Young Lee[1], In-Jae Lee[1], Ji-Won Kim[1], Jung-Hwan Chang[1],
Do-Hyun Kang[1], Shi-Uk Chung[1], and Jung-Pyo Hong[2]

[1] Transverse Flux Machine Research Group, Korea Electrotechnology Research Institute, Korea
[2] Dept. of Automotive Engineering, Hangyang University, Korea
E-mail:jylee@keri.re.kr, linjae@keri.re.kr, and Hongjp@hanyang.ac.kr

Abstract—Most of Contactless Power Transfer Systems (CPTS) have independent structure to improve power transmission efficiency. Sometimes, however, CPTS needs to be a part of moving system to reduce overall system volume. Therefore, this paper proposes a CPTS combined with a linear electric machine loading robots. A prototype CPTS has been constructed for testing and performance evaluation. This paper examines the performance of the prototype by simulation and test with AC-voltage source and PWM-voltage source.

I. INTRODUCTION

Conventional power supply system drags long power cables directly to transfer power and produces many particles because of mechanical friction between power cables and surface of the nearby instruments whereas Contactless Power Transfer System (CPTS) delivers electrical power to load with the help of contactless transformer that has no mechanical contact. In this method, CPTS doesn't produce particles, thereby making it adaptable to the industry applications where clean circumstances are needed such as semi-conductor, LCD, and PDP manufacturing factory [1].

Many kinds of CPTS have been proposed recently, supplying mobile loads and used in flexible power supply systems. Most of these systems use transformers with extended primary windings to transmit power contactlessly from the primary to the secondary. The several examples are introduced in [2]. The great many of these systems have independent structure to improve power transmission efficiency, and the structural characteristics are using ferrite core or having large air-gaps [1-4].

Sometimes, however, CPTS needs to be a part of moving system to reduce overall system volume, and to satisfy this purpose this paper proposes a CPTS combined with a linear electric machine loading robots. A prototype CPTS has been constructed for testing and performance evaluation, and it was introduced in [5] briefly by one of these authors. For research term, the winding was changed and the characteristics were analyzed in more detail.

In the first chapter the basic configuration of the prototype and its magnetic and electric circuit models are introduced. In the next chapter the methods of operation are explained, and one method is selected to operate the prototype in the test. Then, the performance of the prototype is examined by simulation and test with AC-voltage source and PWM-voltage source. Now the proposed CPTS is at development stage, so how much power is transferred is a matter of the concern. The characteristics of the prototype are evaluated in a point of the concern.

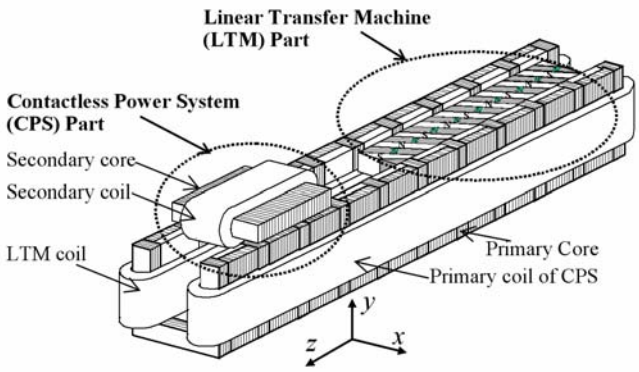

Fig. 1. Configuration of the proposed contactless power transfer system (CPTS) combined with a linear electric machine

II. SYSTEM CONFIGURATION AND ANALYSIS MODELS

A. Configuration

Fig. 1 shows the proposed CPTS combined with electric machine. The linear transfer machine (LTM) is a PM type transverse flux linear machine (TFLM), and the stator functions an additional role as a primary part of the CPTS. The stator core is a primary core for CPTS, and the stator coil can be the primary coil of CPTS or separated from the coil of CPTS as shown in Fig. 1. The secondary of CPTS and mover of TFLM are linked by base frame loading robot structures. The air-gap length of CPTS is relatively small in comparison to other power transfer systems, and the core is iron core. The detail specifications are listed in Table 1.

B. Electric and Magnetic Models

To simulate the CPTS, the transformer equivalent circuit is used as an electric model [5]. The simulation is performed by a commercial program, PSIM with the transformer equivalent circuit as shown in Fig. 2. The necessary

parameters for simulation are listed in Table 2. For the load, resistance is only considered.

If all parameters are measured, the simulation results using the parameters are very reliable. However, it is difficult to measure magnetic and leakage inductances separately. The inductances are calculated from the linkage flux obtained by magnetic field analysis using a 3-dimensional Equivalent Magnetic Circuit Network (3D EMCN) method [6] considering magnetic nonlinearity and 3D magnetic path. The accuracy of the analysis results by the method for TFLMs has been already proved in [6]. Fig. 3 shows the magnetic models of CPTS system.

The leakage inductance of the primary winding is calculated by the linkage flux of MMF1 section of the model m1 and m3. When the leakage inductance of the secondary winding is calculated by the experimental equation in [6], the value is very small as much as can be ignored. The magnetizing inductance is calculated by the linkage flux of MMF2 section of the model m2. The calculated inductances are listed in Table 2.

TABLE I
SPECIFICATIONS OF THE PROTOTYPE CPTS

Material	Conductor of the primary winding	1 x 3	mm^2
	Conductor of the secondary winding	ϕ 1	mm
	Core in the primary	S12	0.35t
	Core in the secondary	S12	0.35t
	Core in the mover	S20C	solid core
	PM in the mover	1.2	T
Dimension	Length of the primary	1360	mm
	Length of the secondary	160	mm
	Length of the mover	160	mm
	Length of the airgap	1	mm

Note) 0.35t = thickness is 0.35mm

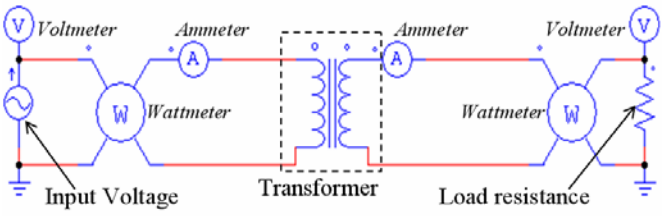

Fig. 2. Transformer equivalent circuit for CPTS simulation

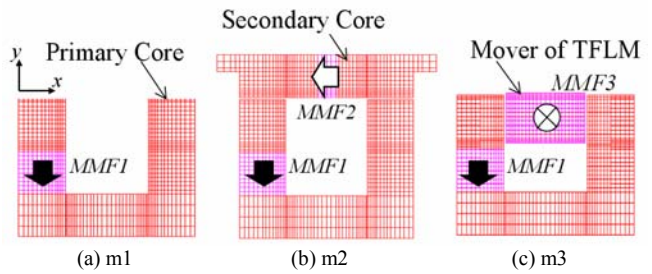

(a) m1 (b) m2 (c) m3

Fig. 3. Meshed analysis models for 3D EMCN analysis : (a) m1 : primary core model, (b) m2 : primary core and secondary core model, (c) m3 : primary core and mover of TFLM model
(MMF1 : magneto-motive force of the stator or primary winding
MMF2 : magneto-motive force of the secondary winding
MMF3 : magneto-motive force of the PM in the mover)

TABLE II
PARAMETERS FOR CPTS SIMULATION

Symbol	Meaning	Value	
		Calculated	Measured
Vp	Input voltage of primary winding (AC source / PWM source)		70Vrms / 300Vpeak
Rp	Resistance of the primary winding	1.24 Ω	***1.21*** Ω
Rs	Resistance of the secondary winding	1.42 Ω	***1.41*** Ω
Lp	Leakage inductance of the primary winding	***22.4*** mH	-
Ls	Leakage inductance of the secondary winding	$\boldsymbol{10^{-6}}$ mH	-
Lm	Magentizing inductance (referred to the primary)	***12.7*** mH	-
Np	No. of turns of the primary winding	-	78 turn
Ns	No. of turns of the secondary winding		143 turn
R_L	Resistance of the load	Variable (10, 20, 40 Ω)	

III. METHODS OF OPERATION

The methods of operation are classified into two: static operation and dynamic operation. This classification is according to movement of CPTS.

A. Static Operation

In static operation, the CPTS is working at standstill. When the mover of TFLM is going and return, the mover speed is zero at turning points. The time of standstill is variable depending on application systems. The CPTS can be working at this time to charge a battery, and the robot or electric system on the mover can be operated by the battery source.

While the CPTS is operating, the mover is stopped. That means the current of stator winding for TFLM is zero. With the same coil, the two systems – TFLM and the CPTS- can be operated in sequence. Since the CPTS is operated independent of TFLM, CPTS is considered as a transformer with airgap.

The most difference from general transformers with airgap is that the CPTS is operated by PWM-voltage source. If TFLM is driven by pure AC-voltage source, the CPTS can be operated by the source in sequence. However, most electric machines including TFLM are driven by PWM-voltage source, and the CPTS should be operated by the same driver in order to save driver cost.

In this paper, the prototype of CPTS is operated by AC power supply to compare the test results with the simulation results of the circuit shown in Fig. 2. Then the prototype of CPTS is also operated by full-bridge converter to test under the real application cases. These simulated and test results are shown in the next chapter.

B. Dynamic Operation

Dynamic operation is that the CPTS is working while the mover is moving. In this case, the frequency of input voltage or current is influenced by switching frequency of stator current of TFLM. If the input frequency of the CPTS is high, the core losses become bigger. So, it is a future work that operating the CPTS at the same frequency of stator current.

IV. ANALYSIS AND EXPERIMENTAL RESULTS

A. *Results by AC-voltage source*

Fig. 4 shows the analysis and measured currents and powers according to load resistance and input frequency variation. The input voltage and current of primary winding are called here primary voltage and primary current respectively. The voltage and current of load resistance are considered as voltage and current of secondary winding, and they are called here secondary voltage and secondary current respectively.

The primary voltage is 70 Vrms, and it is supplied by AC power supply. The primary current is reduced depending on frequency increment because the primary voltage is constant and impedance is increasing according to frequency. At the same frequency, the current and power are decrease depending on resistance increment. It is the same reason as decreasing current according to frequency. The simulation results agreement well with measured results for the primary winding.

In contrast to primary, there are conspicuous errors between simulation and measured results for the secondary winding. The main reason of the errors can be that the core-loss is not considered in the simulation. To reduce the errors, the simulation circuit can be compensated by core-loss resistance such as the circuit in [7].

However if a constant core-loss resistance is used for the circuit, some errors are still remained. If variable core-loss resistances are used according to frequencies and currents, lots of efforts are required. Without considering core-loss, the variation aspect of secondary current and power are well estimated. Therefore at the development stage, the circuit as shown in Fig. 2 or referred in [5] is useful to simulate the characteristics of the CPTS.

As mentioned at Introduction chapter, how much power is transferred is a matter of the concern for the CPTS in this developing stage. That means the maximum secondary power rather than maximum transfer ratio or efficiency. In consequence of simulation and experiment results, the maximum secondary power can be obtained by higher primary power (input power), lower frequency, and lower resistance of load.

Fig. 5 shows the analysis and measured voltages and currents at resistance of load 10 Ohm and the frequency 100Hz. It is one point of each graph in Fig. 4. When the magnitude and phase of voltages and currents are compared in the time domain, it is confirmed again that the measured and simulated results are very agreement.

The magnitude difference between primary and secondary is due to storage power in airgap and core losses [8], and the phase difference is due to impedance difference. Since large resistance is considered as a load in the secondary, the power factor of secondary is almost 1.

B. *Results by PWM-voltage source*

Fig. 6 shows the measured voltages and currents in the time domain when the CPTS is operated by PWM-voltage source supplied by the full-bridge converter.

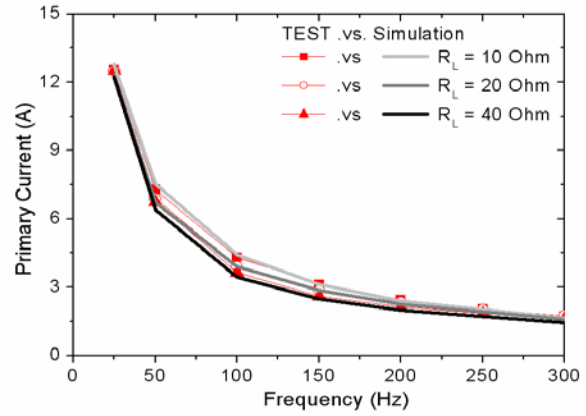

(a) primary current

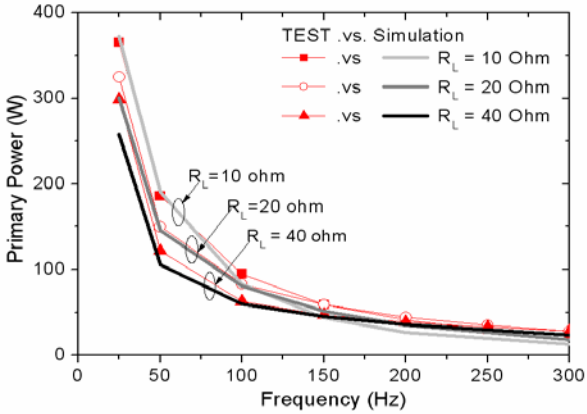

(b) primary power

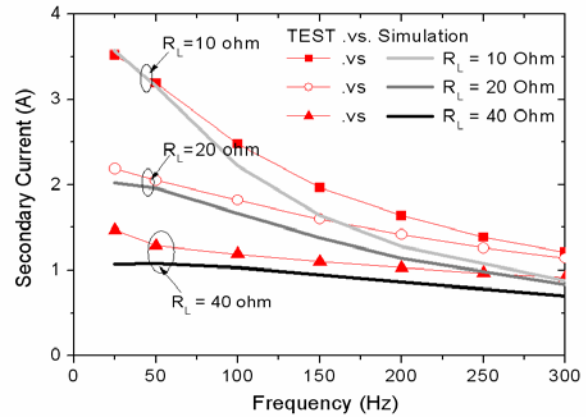

(c) secondary current

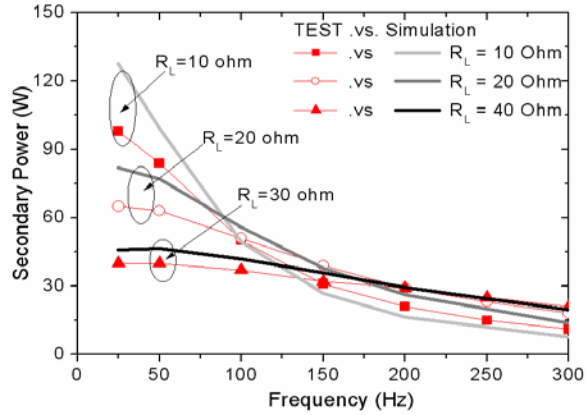

(d) secondary power

Fig. 4. Measured and simulated results by AC-voltage source for resistance of load and frequency variation at constant primary voltage (R_L is resistance of load)

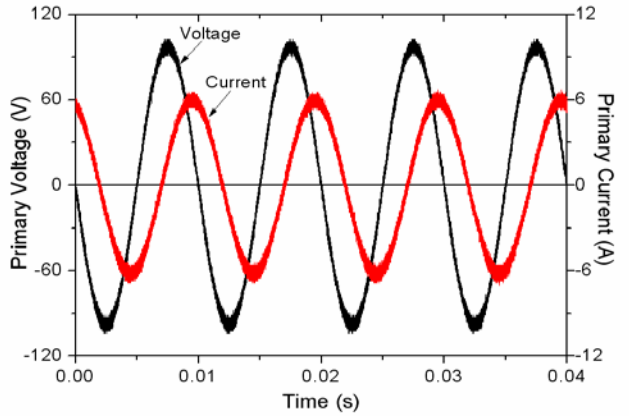

(a) measured values of primary

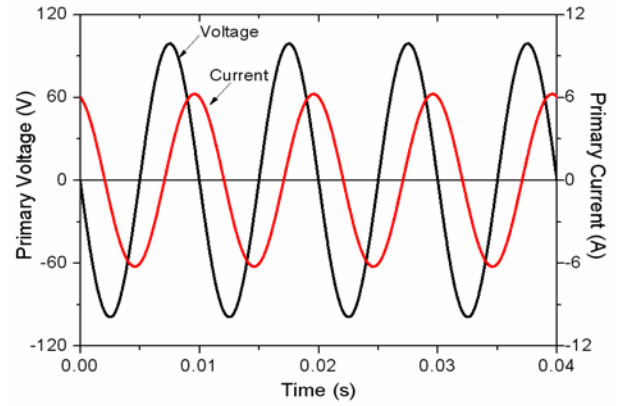

(b) simulated values of primary

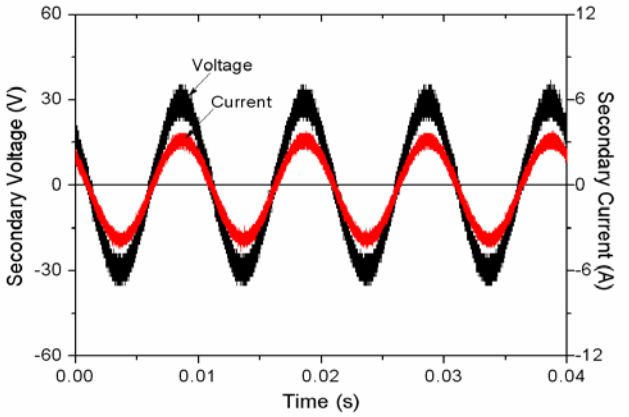

(c) measured values of secondary

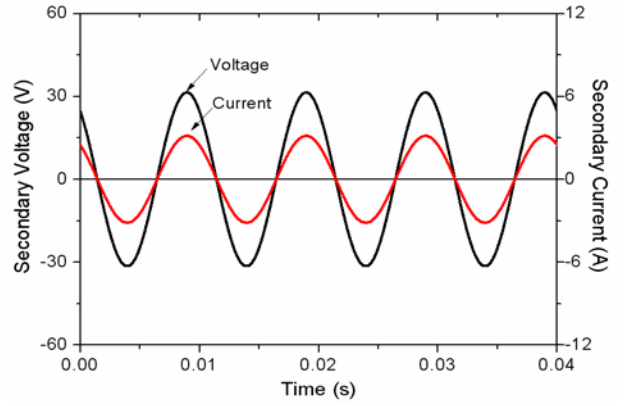

(d) simulated values of secondary

Fig. 5. Measured and simulated results by AC-voltage source at resistance of load 10 Ohm and frequency 100Hz

The Fig. 6 (a) is the results at resistance of load 10 Ohm and the frequency 100Hz. Although the reference primary current is 5A, the measured primary current is 4.7A. Since the primary current is 4.3A in Fig. 5, the results of Fig. 6 (a) can be compared with the results of Fig. 5 under the almost same condition. If the primary current is sinusoid by the PWM voltage, the secondary voltage and current are also sinusoid. Further more, the voltage and current are the same as those obtained by AC power supply test except harmonics.

The Fig. 6 (b) is the results at resistance of load 10 Ohm, the frequency 100Hz, and the reference primary current is 20A. As compared with the condition of Fig. 6 (a), only the reference primary current is increased. Since the peak voltage of PWM is limited to 300V and the inductance of primary winding is large considering converter system, the primary current can not be sinusoidal wave. When the primary current is not sinusoid, the secondary voltage and current waves are also distorted.

The Fig. 6 (c) is the results at resistance of load 10 Ohm, the frequency 300Hz, and the reference primary current is 20A. As compared with the condition of Fig. 6 (b), only frequency is increased. Since in the Fig. 6 (b) the condition already exceed the limit of control capacity, the primary current can reach to the reference value in the condition of Fig. 6 (c) because the electro-motive force (emf) and impedance are higher at the higher frequency.

Fig. 7 shows the measured results for resistance of load and frequency variation. The primary voltage is 300 Vpeak, and it is supplied by full-bridge converter. By the current control, the primary voltage is variable to keep the constant current. The primary reference current is 20A, and the results of Fig. 6 (b) and Fig. 6 (c) are the points on the Fig. 7.

In comparison with the results by AC-voltage source in Fig. 4, the results by PWM-voltage source in Fig. 7 have breakpoints at low frequency. This aspect is similar to the results in [5] which are also obtained by the same converter source. It is the reason of voltage and current wave distortion. At the low frequency such as 50Hz, the current is sinusoid like Fig. 6 (a). However at the higher frequency such as 100Hz, the voltage wave is changed into square wave for current control, and the current wave is distorted like Fig. 6 (b), and it causes voltage and power increment. After voltage saturation, the current is reduced at the higher frequency such as 200~300Hz, and it causes power decrement like Fig. 6 (c).

In consequence of experiment results above, the aspects of secondary characteristics are depending on the aspects of primary characteristics. And if there is no voltage limit, the results by PWM-voltage source are the same as the results by AC-voltage source. That means the maximum secondary power can be obtained by higher primary power (input power), lower frequency, and lower resistance of load.

V. CONCLUSIONS

This paper dealt with the prototype of CPTS combined with TFLM. The CPTS is very different from general transformers or other contactless converter systems in aspects of having air-gap and iron cores, driven by PWM-voltage at low frequency. Further more, the leakage inductance is very large

because the primary winding is the stator winding of TFLM. A resonance circuit to improve transferring power cannot be considered in these conditions. Therefore, the characteristics of CPTS are analyzed by the comparison of the results of simulation and experiment according to operating condition. In conclusion, the maximum secondary power can be obtained by higher primary power (input power), lower frequency, and lower resistance of load if the input voltage is not limited. With the full-bridge converter, the maximum secondary power is 823W in one CPTS. When TFLM is two phase, the secondary power can be about 1.6kW by the tow CPTS.

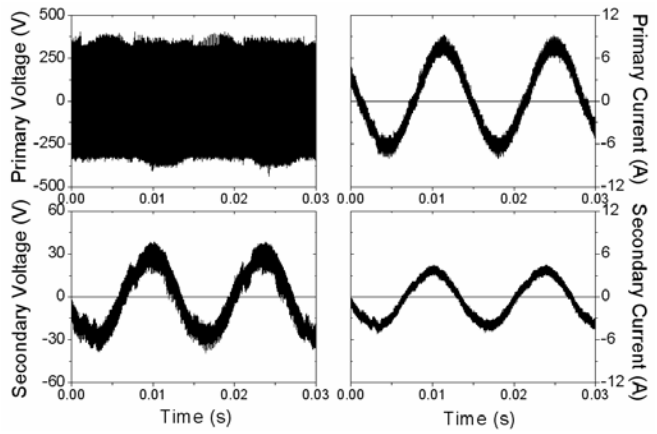

(a) Iref = 5A, f = 100Hz, R_L = 10 Ohm

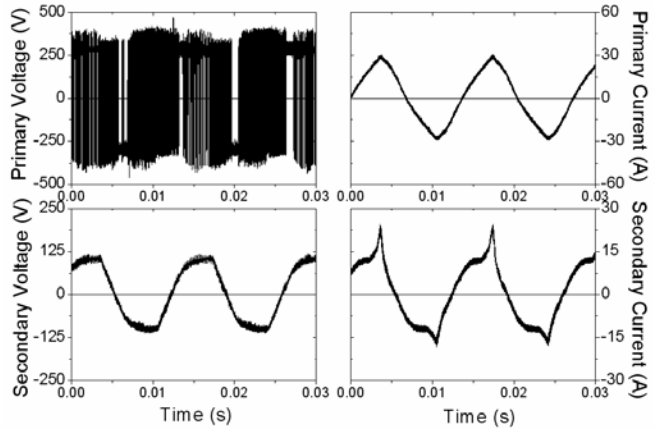

(b) Iref = 20A, f = 100Hz, R_L = 10 Ohm

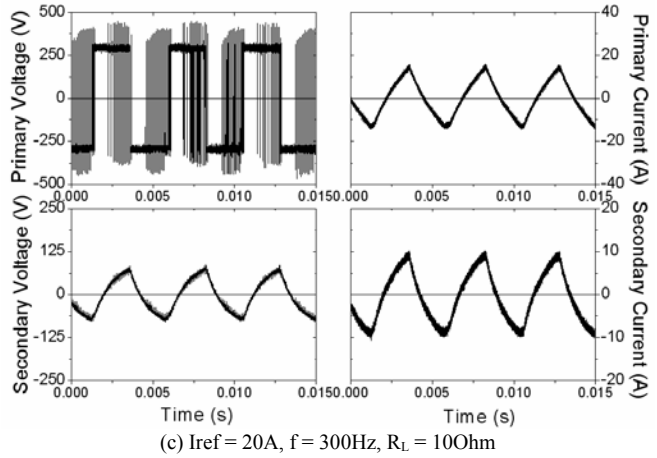

(c) Iref = 20A, f = 300Hz, R_L = 10Ohm

Fig. 6. Measured results by PWM-voltage source
(Iref is reference current value of primary winding, f is frequency, and R_L is resistance of load)

REFERENCES

[1] Myunghyo Ryu, Honnyong Cha, Yongwan Park, and Juwon Baek, "Analysis of the Contactless Power Transfer System using Modeling and Analysis of the Contactless Transformer," *IECON2005*, 32nd Annual Conference of IEEE, pp.1036-1042, November 2005

[2] Jacobus M. Barnard, Jan A. Ferreira, and Jacobus Daniel van Wyk, "Sliding Transformers for Linear Contactless Power Delivery," *IEEE Transactions on Industrial Electronics*, vol.44, No.6, pp.774-779, December 1997

[3] Albert Esser and Hans-Christoph Skudelny, "A New Approach to Power Supplies for Robot," *IEEE Transactions on Industry Applications*, vol.27, No.5, pp.872-875, September/October 1991

[4] Shin-ichi, Fumihiro Sato, Shinki Kikuchi, "Consideration of Contactless Power Station with Selective Excitation to Moving Robot," *IEEE Transaction on Magnetics*, vol.35, No.5, pp.3583-3585, September 1999

[5] Jong Moo Kim, Do Hyun Kang, Soo Jin Jung, and Deok Je Bang, "Design of the Transverse Flux Linear Motor with the Integrated Contactless Power Supply," *5th LDIA2005*, pp.286-289, September 2005

[6] Ji-Young Lee, Jung-Pyo Hong, Jung-Hwan Chang, and Do-Hyun Kang, "Computation of Inductance and Static Thrust of a Permanent-Magnet-Type Transverse Flux Linear Motor," *IEEE Transactions on Industry Application*, vol.42, No.2, pp.487-494, 2006

[7] E.F.Fuchs, M.A.S.Masoum, D.J.Roesler, "Large Signal Nonlinear Model of Anisotropic Transformers for Nonsinusoidal Operation, Part I; λ-I Characteristic," *IEEE Transactions on Power Delivery*, vol. 6, No. 1, January 1991.

[8] John D. Ramboz, "A High Accurate, Hand-Held Clamp-on Current Transformer," *IEEE Transactions on Instrumentation and Measurement*, vol. 45, No. 2, pp 445-448, April 1996

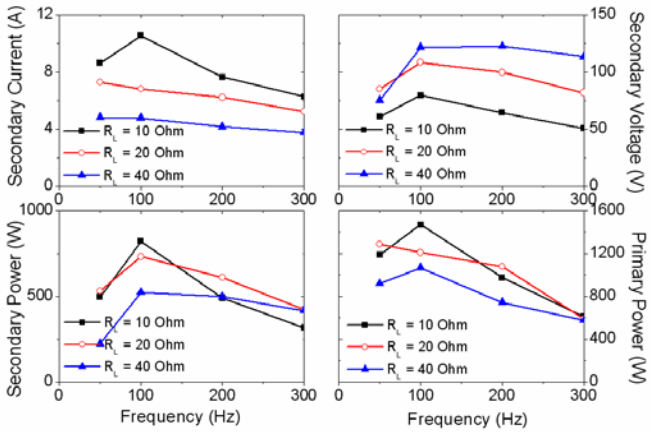

Fig. 7. Measured results by PWM-voltage source for resistance of load and frequency variation at constant primary reference current, 20A (R_L is resistance of load)

International Conference on Electrical Machines and Systems 2007

October 8 ~ 11, Seoul Olympic Parktel, Seoul, Korea

Information about how to order the publication :

KIEE (The Korean Institute of Electrical Engineers)
Room 901, Science & Technology Building, 635-4, Yucksam-Dong, Kangnam-Ku, Seoul
135-703 Korea

Tel: +82-2-553-0151 Fax: + 82-2-566-9957 E-mail: kiee@kiee.or.kr

Organized by

KIEE (The Korean Institute of Electrical Engineers)

Co-organized by

CES (China Electrotechnical Society)

IEEJ (The Institute of Electrical Engineers of Japan)

Technical Co-sponsor

IEEE IEEE Industry Application Society

IEEE Catalog Number : 07EX1815C
ISBN Number : 978-89-86510-07-2
Vendor : Prof. Guee Soo Cha
Tel : +82-41-530-1334 Fax : +82-41-530-1548
E-mail : gsoocha@sch.ac.kr

Oral Presentation 2 Oct, 10, 2007 (Wed,) 13:30-17:50

· SM2-01	**Self-sensing of the Rotor Position and Displacement for an Inset Permanent Magnet Type Bearingless Motor** Heng Nian, Yikang He, Dong Chen, Lei Huang	
· SM2-02	**Short-Armature Self-Excitation Type Linear Synchronous Motor for Transport System** Tsuyoshi Higuchi, Takashi Abe, Jun Oyama, Takashi Yoshida, Tadashi Hirayama	
· SM2-03	**Performance of Flux Reversal Motor at Various Rotor Pole Arcs** Pranshu Upadhyay, N. K. Sheth, K. R. Rajagopal	
· SM2-04	**Design Study of High-Temperature Superconducting Motors for Ship Propulsion Systems** Naoki Maki, Mitsuru Izumi, Masayoshi Numano, Kiyoshi Aizawa, Kagao Okumura, Katsunori Iwata	
· SM2-05	**Small-Scale Tubular Linear Induction Motor for Pneumatic Capsule Pipeline System** Wisuwat Plodpradista	
· SM2-06	**Maximum Power Point Tracking Control and Voltage Regulation of a DC Grid-Tied Wind Energy Conversion System Based on a Novel Permanent Magnet Reluctance Generator** Kazmi Syed Muhammad Raza, Hiroki Goto, Hai-Jiao Guo, Osamu Ichinokura	
· SM2-07	**Static Characteristic of a Novel Dual-Stator Hybrid Excited Synchronous Generator Based on 3D Finite Element Method** Liu Xiping, Lin Heyun, Yang Chengfeng, Fang Shuhua, Guo Jian	
· SM2-08	**Contactless Power Transfer System Combined with Linear Electric Machine** Ji-Young Lee, In-Jae Lee, Ji-Won Kim, Jung-Hwan Chang, Do-Hyun Kang, Shi-Uk Chung, Jung-Pyo Hong	
· SM2-09	**Design of Electromagnet for High Levitation Force in 3D Superconducting Actuator** Jin-Hong Joo, SeokBeom Kim, Kei Hitomi, Satoru Murase	
· SM2-10	**Performance Analysis of an SMC Transverse Flux Motor with Modified Double Sided Stator and PM Flux Concentrating Rotor** Youguang Guo, Jianguo Zhu, Haiyan Lu, Shuhong Wang, Jianxun Jin	
· SM2-11	**Voltage Control and Hysteresis Current Control of a 8/6 Switched Reluctance Motor** P. Srinivas, P.V.N. Prasad